Version of Record: https://www.sciencedirect.com/science/article/pii/S0165783620302708
Manuscript_34722c0e182e7537fc2460efc9c22fd0

Estimation of growth parameters integrating tag-recapture, length-frequency, and direct aging data using likelihood and Bayesian methods for the tropical deepwater snapper Pristipomoides filamentous in Hawaii

Scherrer, Stephen R.[1]*, Kobayashi, Donald R.[2], Weng, Kevin C.[3], Okamoto, Henry Y.[4], Oishi, Francis G.[4], Franklin, Erik C.[5]

[1]University of Hawaii, Oceanography Department, 1000 Pope Rd, Honolulu, Hawaii 96822, scherrer@hawaii.edu
[2]National Marine Fisheries Service, Pacific Islands Fisheries Science Center, 1845 Wasp Blvd, Honolulu, Hawaii 96818, donald.kobayashi@noaa.gov
[3]Virginia Institute of Marine Science, College of William and Mary, 1375 Greate Road, Gloucester Point, Virginia 23062, kevinweng@vims.edu
[4]Division of Aquatic Resources, State of Hawaii Department of Land and Natural Resources, 1151 Punchbowl Street, Room 330, Honolulu, Hawaii 96813
[5]University of Hawaii, School of Ocean and Earth Science and Technology, Hawaii Institute of Marine Biology, 46-007 Lilipuna Rd, Kaneohe, Hawaii 96744
erik.franklin@hawaii.edu

*Corresponding author

Abstract

Pristipomoides filamentosus is an economically and culturally important species of deepwater snapper found throughout the tropical Indo-Pacific. From 1989 to 1993, the State of Hawaii initiated a tagging program with fish opportunistically recaptured by scientists and fishers to quantify growth and other life history parameters for the species. Over approximately 10 years, 10.5% of the 4,179 tagged fish were recaptured. We used these data to compare von Bertalanffy growth parameters estimated using Bayesian and likelihood approaches. Next, we defined an objective cost function to estimate growth parameters that integrated the tagging data with direct aging and length frequency data used in previous regional growth studies. Our results reconcile 30+ years of effort from various methods to estimate growth parameters for *P. filametosus* in Hawaii (L_∞=68.14 cm FL [95% Confidence Interval (CI): 65.42–69.54] and K=0.22yr^{-1} [CI: 0.20–0.25]), demonstrate the importance of individual variability in the species due primarily to the asymptotic length parameter L_∞, and suggest the effects of sexual dimorphism on growth as a focus of future inquiry. These results have direct management implications as growth is a critical input for age-based stock assessment models and often used as a proxy for other life history traits.

* Corresponding Author

1. Introduction

Pristipomoides filamentosus (Valenciennes, 1830) is a species of long-lived deepwater snapper distributed throughout the tropical Indo-Pacific (Allen, 1985; Gaither et al., 2011). The species constitutes a significant fraction of Hawaii's commercial bottomfish fishery where it is colloquially known as opakapaka (Ralston and Polovina, 1982; Langseth et al., 2018). *P. filamentosus* is one of seven management unit species pooled for the assessment of Hawaii's bottomfish stock. However, there is interest in the potential use of species-specific, age-structured assessments for this stock, which require accurate estimates of growth and other life history parameters (Langseth et al., 2018; Maunder et al., 2015, Oyafuso et al. 2017).

Several studies have used different approaches to estimate growth parameters for *P. filamentosus* in Hawaii and elsewhere in the Indo-Pacific (Table 1). Early estimates were obtained using direct aging approaches with length-at-age data from otolith reads interpreted as a proxy for age (Ralston and Miyamoto, 1983; Uchiyama and Tagami, 1984; Radtke, 1987; DeMartini, et al., 1994, Ralston and Williams, 1988). These methods relied on the integration of daily otolith bands which can bias age estimates due to episodic growth and poor increment resolution in early (< 5 years) life stages (Wakefield et al., 2017). Revised parameter estimates using the direct aging approach were obtained by supplementing datasets from those earlier studies with additional length-at-age data where ages were estimated using bomb radiocarbon and lead-radium ratios (Andrews et al., 2012). In addition, a length frequency approach was used to estimate growth parameters by tracking the modal length progression of juvenile cohorts caught in nursery habitat in Kaneohe Bay, Hawaii. However, this study used a previous estimate of L_∞ where individual variability was not considered; this omission can result in biased parameter estimates (Sainsbury, 1980, Moffitt and Parrish, 1996). Estimation of growth parameters from an ongoing mark-recapture study (separate from the results reported here) has attempted using growth increment approaches, but preliminary results have been limited by the size distribution of recaptured individuals and the use of a parameterization of von Bertalanffy's growth function (VBGF) that is not compatible with direct aging and length frequency approaches (Francis, 1988a; O'Malley, 2015). While the methods of each of the aforementioned studies produced individual estimates of growth parameters, none of the studies attempted to integrate all three classes of data (i.e., direct aging, modal progression, growth increment from tagging) to explicitly evaluate the parameter values and sources of uncertainty.

Analytical and statistical advances for estimating growth have developed to account for sources of variability and permit parameter comparisons across length-at-age, length frequency, and tagging based approaches (Eveson et al., 2004; Francis, 1988b; Wang et al., 1995). Structural modifications to Fabens (1965) parameterization of the VBGF address issues of compatibility between growth parameters from direct aging and length frequency approaches with those derived from tagging studies (Maller and Deboer, 1988; James, 1991; Palmer et al., 1991, Laslett et al., 2002; Eveson et al., 2004, 2007; Zhang et al., 2009). These methods use maximum likelihood and Bayesian frameworks to accommodate individual variability by describing population parameters using probability distributions (Francis, 1988b; Kimura et al., 1993; Wang et al., 1995; Zhang et al., 2009). Bayesian approaches allow K and L_∞ to be sampled in this manner and can account for prior information when estimating parameters (Zhang et al., 2009). Maximum likelihood approaches typically estimate K once for the entire population (henceforth referred to as "fixed") but flexibility in their implementation has allowed for the development of model structures that can estimate a single set of growth parameters from direct aging, length frequency, and growth increment data simultaneously (Wang et al. 1995, Laslett et al. 2002, Eveson et al. 2004).

We derive growth parameters using Bayesian and maximum likelihood methods applied to a previously unreported dataset from a cooperative tagging program for *P. filamentosus* in the Main Hawaiian Islands (MHI), with fishers opportunistically recapturing fish and reporting to the State of Hawaii's Division of Aquatic Resources. Parameters estimated from these data using a Bayesian framework are compared to a maximum likelihood approach integrating tagging data with length-at-age and length frequency data previously used to describe growth in *P. filamentosus* in the MHI and Northwestern Hawaiian Islands (NWHI). These new growth estimates are compared to those previously reported for *P. filamentosus* in the Hawaiian Archipelago.

2. Materials and methods

2.1 Opakapaka tagging program

Tagging data used for this analysis were obtained by biologists from Hawaii's Division of Aquatic Resources (DAR) within the state's Department of Land and Natural Resources (DLNR). Between 1989 and 1993 the Opakapaka Tagging Program (OTP), led by staff biologist Henry Okamoto operated from fishing vessels contracted out of Honolulu Harbor, tagging and releasing 4,179 *P. filamentosus* in total. All tagging occurred in the MHI, with coarse location data for the site of tagging and recapture recorded using the commercial statistical reporting grid (Table 2; Figure 1). Tagging effort concentrated primarily around the island of Oahu and the Maui Nui complex which includes the islands of Maui, Molokai, Lanai and Kahoolawe. Since 1990, these areas have accounted for approximately 67.7% of Hawaii's commercial bottomfish harvest. Fewer than 1% of fish in this study were tagged offshore of the islands of Niihau and Hawaii (Big Island).

Fish were caught with hook-and-line gear and brought to the surface at a rate of 2-5 feet per second. Prior to tagging, each fish was placed in a holding container with aerated seawater to assess their likelihood of surviving. Fish appearing lively and upright were deemed suitable candidates for tagging. If the stomach was inverted and full of gas, it was punctured using a small sharp instrument (e.g., scalpel, hypodermic needle, fishhook). A few scales were removed and a small surgical incision (~1 cm) was made near the fish's anal opening to assist in expelling gas from the body cavity. A uniquely identifiable monofilament streamer tag was anchored within and protruded from this incision. The fork length of each fish was recorded to the nearest ¼ inch in addition to the location and time of capture before returning the fish to the to sea headfirst with downward momentum attempting to counteract buoyancy due to any residual gas (Okamoto, 1993).

Local commercial and recreational fishers were made aware of the program through fliers distributed at the local fish markets, to fish dealers, at fishing supply outlets, and posted at small boat harbors and recaptured fish were reported up to a decade after they were tagged (Kobayashi, 2008; Okamoto 1993). Fishers were incentivized with a $10 reward to report the date, location, and depth that each fish was landed and the fish's fork length. When recaptured by OTP personnel, tagged fish were fitted with an additional tag and released again.

2.2 Tagging data management

The data collected by the OTP were entered into a spreadsheet and subsequent analysis was performed using R (R Core Team, 2014), the Bayesian statistical software JAGS (Plummer, 2003), and the R package R2Jags (Su and Yajima, 2012). The dataset was filtered to remove records of individuals that were never recaptured, individuals for which the tagging date, recapture date, or tag ID was not recorded, and individuals that were not the species of interest. Fork lengths for the remaining fish recorded at tagging and recapture were linearly transformed from inches to centimeters prior to model fitting for consistency with growth parameters estimated elsewhere. Incremental growth (Δl) and time at liberty (Δt) were calculated for each fish. When individuals were recaptured on more than one occasion, Δl and Δt were only calculated between the first marking event and the final recapture so as to not violate model assumptions of independence. Fish with Δt less than 60 days were excluded from the dataset.

2.3 Parameter estimation from tagging data: Bayesian approach

Growth parameters were estimated for the *P. filamentosus* tagging data following the Bayesian methodology of Zhang et al. (2009). This approach uses a Fabens version of the VBGF but allows the parameters to vary among individuals. Hence the predicted length of a captured individual is expressed as:

$$L_i = L_{\infty,i}(1 - e^{-K_i(A_i+\Delta t_i)}) \tag{1}$$

This equation is parameterized such that $L_{i,j}$ is the length of individual i when the individual is captured (that is, when an individual is initially captured and marked and again during the final recapture event), Δt_i is the time-at-liberty (time between initial capture and the last recapture) for the *ith* individual when it was recaptured. This term is zero when the equation is used to calculate the individual's length at capture. A_i is the relative age of *ith* individual at tagging (age minus Δt_i). Parameters K and L_∞ are the VBGF parameters for the *ith* individual drawn from Gaussian distributions defining the population means. Moderately informative normally distributed priors for K and L_∞ were constructed from the mean and variance of each parameter previously estimated by other regional studies [$K \sim N(0.242y^{-1}, 0.114)$ and $L_\infty \sim N(71.4cm, 24.7)$] (Table 1). Uninformative priors were used for all other parameters, following the approach of Zhang et al. (2009).

The hierarchical Bayesian model allowed both the K and L_∞ parameters to vary among individuals by sampling these parameters from the distribution of hyperparameters, as described above is henceforth referred to as Model 1. This model was compared to three additional models fit with various constraints to K and L_∞. Model 2 estimated the K parameter once for the entire population (henceforth referred to as "fixed") while accounting for variation among individuals by sampling L_∞ from hyperparameter distributions. Model 3 treated L_∞ as a fixed parameter while sampling K parameter from hyperparameter distributions, and both parameters were fixed under Model 4.

Evaluating the restrictive assumptions of models 2-4 was accomplished by comparing growth parameters to those estimated using Model 1. Model 1 is the presumptive best estimate for *P. filamentosus* VBGF parameters, since it allows the most flexible incorporation of individual variability by sampling both L_∞ and K from hyperparameters. If a given parameter is relatively stable when the parameter varies across individuals and when it was treated as fixed for the population, then it might be inferred that treating this parameter on an individual basis is not warranted. However, if parameter estimates differed when the parameter was fixed, then it might be inferred that treating this parameter on an individual basis is necessary. Model 4 would *a priori* be most similar to the Fabens approach, with both fixed K and L_∞, but with the added feature of estimating ages at initial tagging, A_i. It is the inclusion of this term that models growth as a function of age, rather than length, allowing for direct comparison between parameters estimated using tagging data and those obtained from direct-age and length frequency approaches (Wang et al., 1995).

For each Bayesian model, the first 150,000 samples from the posterior distribution were treated as burn-in and discarded from the Monte Carlo simulation. Additional samples were thinned at an interval of 1/50 (number kept = 30,000) to reduce potential autocorrelation between sequential values or strings of values in the posterior distributions. Initial starting estimates of K and L_∞ were obtained from Andrews et al. (2012) with two additional chains run simultaneously with initial starting values 50% lower and 100% higher. This resulted in nearly identical solutions as shown in Table 3. The mean K and L_∞ values from the posterior distribution were used as metrics of population values. Median values deviated from mean values by less than 0.5% (Table 3), indicative of symmetrical distributions easily characterized by any descriptor of value tendency (i.e., mean, median, or mode). Convergence was also ascertained by examination of the Gelman-Rubin statistic (Gelman and Rubin, 1992).

The fit of each model was assessed by calculating a Bayesian p-value from the posterior predictive distribution. Bayesian p-values were simulated using the model's posterior distribution and test whether simulated data are more extreme than the observed data. Bayesian P-values range between 0 and 1 where values approaching 0.5 indicate the model is a good fit to the data, while extreme values near 0 or 1 indicate that the model does not adequately represent the data (Meng, 1994). The deviance information criterion (DIC) was used to compare models.

2.4 Parameter estimation from tagging data: Maximum likelihood approach

The maximum likelihood approach of Laslett et al. (2002) was used to fit Model 5 according to:

$$l_{ij} = \mu_{\infty}\left(1 - e^{-K(a_i + \Delta t_i)}\right) + \varepsilon_{ij} \quad (2)$$

This method derives growth parameters from the joint distribution of an individual's length at tagging and at recapture. This is most similar in approach to Model 2 of the Bayesian approach in that asymptotic length, L_{∞}, is treated as a normal random effect $N(\mu_{\infty}, \sigma_{\infty}^2)$, accounting for differences among individuals, while K is treated as an unknown fixed parameter. Rather than using length increments to fit observed growth, a bivariate normal joint distribution of lengths recorded at marking and recapture is used to estimate each individual's age at tagging (a_i). The distribution of a_i across all individuals (A) is treated as a random effect with a lognormal distribution $L(\mu_{logA}, \sigma_{logA}^2)$. Measurement error is also treated as a random normal distribution $N(0, \sigma^2)$. An unconditional joint density is then derived for each individual by integrating their individual joint distribution with respect to a. This process is described in greater detail by Laslett et al. (2002).

This approach was used to estimate values of the growth parameters μ_{∞}, σ_{∞}^2, K, $\mu_{\log A}$, σ_{logA}^2, and σ^2 by minimizing of the negative log-likelihood cost function obtained from summing the unconditional joint density $\mathrm{h}(l_1, l_2)$ of each individual, i.e.:

$$-\ln(\lambda_1) = -\sum_i \ln \mathrm{h}\left(l_{m,i}, l_{r,i}\right) \quad (3)$$

Two-sided 95% confidence intervals (2.5%, Median, 97.5%) were estimated for each parameter using a bootstrapping procedure based on 10,000 iterations. During each bootstrap iteration, the model was refit using data randomly resampled with replacement from the original tagging data.

2.5 Estimation of integrated growth parameters using sources of growth data

Datasets previously used in other studies to quantify the growth of *P. filamentosus* in the MHI and NWHI were combined with OTP tagging data to produce a single set of integrated parameter estimates using a modified form of the method proposed by Eveson et al. (2004). Additional datasets that were included represent both direct aging and length frequency approaches and are briefly described below. In total, 6 candidate models (Models 6-11) were fit using this approach (Table 4).

2.6 Parameter estimation: Length frequency data

Length frequency data consisted of the size distributions of juvenile *P. filamentosus* sampled over 13 months between October 1989 and February 1991 as reported by Moffitt and Parrish (1996). The reported fork lengths of captured fish were binned in 1 cm increments and presented in 13 histograms corresponding to each month of sampling. The data were reconstructed by overlaying a series of evenly spaced horizontal lines across the Y-axis of each histogram corresponding to the addition of a single fish. The reconstructed data contained 1,048 observations, one more than was reported by the original study (Moffitt and Parrish, 1996).

The reconstructed length frequency data were incorporated into integrated models by following the two-step method described by Laslett et al. (2004). In the first step, a Gaussian mixture model was fit using maximum likelihood and used to decompose the distribution of fork lengths for each recruitment cohort present for each month of data. This was done using the normalmixEM function from the mixtools package in R (Benaglia et al., 2009) by assuming the mean of each distribution corresponded to the observed mode. A bimodal Gaussian mixture model was fit for the data collected between the months of October-February, as the original study reported that two cohorts were present during this period. A single cohort was present the remainder of the year. In the second step, estimated mean fork length, $\hat{\mu}_{ijk}$, and standard error, s_{ijk}, of each cohort during each month of sampling was used to estimate growth parameters using the following parameterization of the VBGF:

$$\hat{\mu}_{ijk} = \mu_{\infty}\left(1 - e^{-K(a_{ijk} - a_0)}\right) + e_{ijk} + \varepsilon_{ijk} \tag{4}$$

With this parameterization, $i, j,$ and k reflect the fishing year, month, and age cohort, respectively. The estimated age of each cohort at each sampling period is denoted by a_{ijk}. Ages were estimated relative to the month of July when peak spawning of *P. filamentosus* occurs, resulting in age estimates between 3 and 19 months (Luers et al., 2017). Sampling and residual model errors were described using random normal distributions. In contrast to tagging and direct aging methods, length frequency approaches lack the information to estimate the variance component of asymptotic length (L_{∞}), so this term was modeled as fixed effect, μ_{∞}. From this, the expected mean fork length of each cohort (Eqn 6), and associated variability during each sampling period (Eqn 7) were used to minimize the model's negative log-likelihood (Eqn 8). The rationale for these approximations is discussed to greater depth in Eveson et al. (2004).

$$E(\hat{\mu}_{ijk}) = \mu_\infty\left(1 - e^{-K(a_{ijk} - a_0)}\right) \quad (6)$$

$$V(\hat{\mu}_{ijk}) = s_{ijk}^2 + \sigma_\varepsilon^2 \quad (7)$$

$$-\ln(\lambda_2) = \frac{1}{2}\sum_i \sum_j \sum_k \left[\ln\left(2\pi\, V(\hat{\mu}_{ijk})\right) + \frac{(\hat{\mu}_{ijk} - E(\hat{\mu}_{ijk}))^2}{V(\hat{\mu}_{ijk})}\right] \quad (8)$$

2.7 Parameter estimation: Direct aging data

Sources of direct ageing data included four length-at-age datasets from three prior growth studies. Approaches for estimating age differed among studies and included analytical integration of otolith bands (Ralston and Miyamoto, 1983, n = 65), counts of otolith micro increments (DeMartini et al., 1994, n = 35), comparison of otolith derived bomb radiocarbon ratios ($\Delta^{14}C$) relative to a standard reference obtained from hermatypic coral cores from the Hawaiian Archipelago (Andrews et al., 2012, n = 33), and otolith-derived lead-radium ratios pooled by size class (Andrews et al., 2012, n = 3).

The details of the method used to estimate growth parameters from direct aging data are described in detail in Eveson et al. (2004). Briefly summarized, parameters are modeled using the following VBGF parametrization:

$$l_i = l_{\infty i}\left(1 - e^{-K(a_i - a_0)}\right) + \gamma_i \quad (9)$$

Expected length for each individual and the variance of the measurement error is described by equations 10 and 11.

$$E(l_i) = \mu_\infty(1 - e^{-K(a_i - a_0)}) \quad (10)$$

$$V(l_i) = \sigma_\infty^2(1 - e^{-K(a_i - a_0)})^2 + \sigma_\gamma^2 \quad (11)$$

where l_i denotes the length of the i^{th} fish, at age a_i and a_0 is a fixed parameter analogous to t_0 when a fish has a hypothetical length of zero. As with the model for tagging data, $l_{\infty i}$ is the individual asymptotic length of the i^{th} fish drawn from the random normal distribution $L_\infty = N(\mu_\infty, \sigma_\infty)$. γ_i represents the distribution of individual measurement error and is similarly random, drawn from the distribution $\gamma = N(0, \sigma_\gamma)$. The log-likelihood function derived from these equations is described by:

$$-ln(\lambda_2) = \frac{1}{2}\sum_i \left[\ln(2\pi V(l_i)) + \frac{(l_i - E(l_i))^2}{V(l_i)}\right] \quad (12)$$

2.8 Defining an objective cost function and estimating integrated growth parameters

To derive integrated growth parameters across tag-recapture, direct aging, length frequency, and growth increment data sources, we developed an appropriate integrated cost function, defined from the sum of the likelihood functions for each data source and a set of scaling constants, β_i (Eqn 13). The single set of growth parameters best describing all data sources is obtained through minimization of:

$$\Lambda = \beta_1 ln(\lambda_1) + \beta_2 ln(\lambda_2) + \beta_3 ln(\lambda_3) \ldots + \beta_n ln(\lambda_n) \quad (13)$$

Models 6-11 were developed and evaluated by permutating the value of scaling constants, the pooling of datasets using similar approaches, and whether length-at-age data where age estimates were obtained through integration of daily otolith bands were included (Table 4). Two approaches were used for the value of scaling constants (β_i). The first weighted scaling constants for every data source so that each source contributed equally to the resulting parameter estimates while the second weighted each source proportionate to its number of observations. Other differences between integrated models included whether the four direct aging data sources contributed individually to the integrated cost function or if they were first pooled. Omitting direct aging data where ages were estimated by integrating daily growth increments was also considered as this method is likely to underestimate age (Table 4; Wakefield et al., 2017).

2.9 Model evaluation

The six candidate integrated models (Models 6-11) were evaluated using a repeated cross validation procedure to determine the model structure that best predicted the growth observed in the OTP data (Burman, 1989). During each iteration of this procedure, two thirds of fish in the OTP dataset (n = 258) were randomly selected without replacement for model training while the remaining third (n = 129) were used to test model performance. Performance was assessed by the ability of each parameter set, fit using the training data, to predict the expected length-at-recapture for fish in the test data by calculating the root mean squared error (RMSE) between the predicted and observed growth. The preferred model was that which most frequently resulted in the lowest RMSE over 10,000 iterations. To determine if incorporating additional data sources improved predictive performance, RMSE for the preferred integrated model was then compared to the structure of Model 5 which included only tagging data.

Once the structure of the preferred integrated model was determined, two-sided 95% confidence intervals were estimated for each parameter from 10,000 bootstrap iterations. As with tagging data, the procedure for resampling direct aging data involved random sampling with replacement to construct synthetic datasets with an equal number of observations as the original data. Bootstrapping length frequency data was done by hierarchical sampling such that the study periods in each bootstrapped dataset were resampled from the corresponding periods of the original data.

2.10 Sensitivity analysis

The accuracy of growth parameters can be affected by the distribution of individuals sampled relative to that of the total population (Bolser et al., 2018; Calliet and Tanaka, 1990). Gear selectivity, sampling location, variation in annual recruitment, and other factors can lead to under representation of some size and age classes in the sample population and introduce bias to parameter estimates (Goodyear, 2019; Kapur et al., 2020).

There were no records of the gear type used to sample and recapture fish in this study, so it was not possible to directly incorporate this information in the modeling process. Therefore, a sensitivity analysis was performed to quantify the effect of the sampled distribution on parameter estimates with an approach inspired by Bolser et al. (2018). It was not possible to simulate new observations without making assumptions about growth parameters because the growth observed in each individual between marking and recapture events is an essential input to growth increment approaches, so a synthetic dataset was constructed through hierarchical resampling of the original OTP data.

The data were binned by the length of each fish at the time of tagging in 5-cm increments and then observations from each bin were randomly resampled with replacement until each bin contained 200 observations to compensate for uneven sampling across size classes. Each model was then refit using this synthetic dataset. The robustness of each model to the sampling distribution of the data was determined by whether or not the point estimates generated from the sensitivity analysis fell within the previously determined 95% confidence intervals. The influence of the sampling distribution on each model was quantified by the percent difference between parameter estimates for L_∞ and K fit with synthetic data and those fit using the observed data. This type of approach does not explicitly account for differences in selectivity or differences between the sampled and true population structure, but it can fill critical gaps caused by these issues by flattening the number of observations across size classes (Bolser et al., 2018).

3. Results

3.1 Opakapaka Tagging Program

In total, 487 recaptures were recorded for 439 unique individuals for a recapture rate of 10.5% (Table 2). Mortality of fish upon release appeared to be generally low, likely due to the selection of healthy fish in good condition. Some immediate mortality was observed due to capture stress and predation by sharks and cetaceans (4 individuals). Long-term mortality was thought to be relatively low based upon the high rates of tag return spanning many years. Hydra (small cnidarian polyps) biofouling of the tags was observed for some individuals with large times at liberty, and some recaptured fish had lesions apparent where the tag exited the body cavity. This was not thought to be a serious health issue since the fish appeared to be feeding and swimming normally.

Initial fork length at capture across all individuals ranged in size from 16.5 to 53.3 cm (mean = 31.9 cm, standard deviation [s.d.] = 5.5) and ranged from 19.1 cm and 52.8 cm (mean = 32.8, s.d. = 5.1) for fish that were later recaptured. For those fish that were later recaptured, fork length measured at recapture was between 22.9 cm and 76.2 cm (mean = 41.9, s.d. = 8.7). The minimum time at liberty for any fish between tagging and recapture was a single day while the maximum time at liberty was 10.3 years (3,748 days) (Fig. 2). The mean time at liberty was 1.82 years or 666 days (s.d. = 625).

One fish was excluded from further analysis as its initial fork length at capture was not recorded so growth could not be calculated. Seven fish were removed because the recapture date was not properly recorded and therefore their time at liberty could not be determined. Of the remaining 432 fish recaptured, 351 were recaptured a single time, 33 fish were recaptured a total of two times, one fish recaptured 3 times, and two fish were recaptured 4 times. We also excluded from analysis 45 individuals for whom time at liberty was less than 60 days to minimize the influence of any short-term tagging effects. This process yielded records from 387 individuals.

3.2 Estimating growth parameters from tagging data: Bayesian approach

The Bayesian hierarchical approach produced mean estimates of L_∞ and K for Models 1–4 (Table 3). Model 1, which incorporated individual variability in both L_∞ and K, yielded mean parameter estimates of L_∞ = 61.4 cm (coefficient of variation [c.v.] = 2.56) and K = 0.29 yr^{-1} (c.v. = 8.3). L_∞ and K parameter estimates for Model 2, where K was fixed, were 61.8 cm (c.v. = 2.72) and 0.29 yr^{-1} (c.v. = 45.6) respectively. Under Model 3, where L_∞ was fixed and K was fit freely L_∞ = 73.7 cm (c.v. = 41.0) and K = 0.17 yr^{-1} (c.v. = 8.6) and L_∞ = 73.6 cm (c.v. = 42.7) and K = 0.17 yr^{-1} (c.v. = 72.9) for Model 4, where both parameters were fixed. Additional parameters for each of the four models are presented in Table 3. The Gelman-Rubin convergence criteria indicated that the model solutions were credible, with asymptotic convergence clearly occurring after ~4,000 iterations, well within the burn-in phase of the Bayesian modeling runs. All 4 models appeared to fit the the data well; the mean Bayesian P-values from all retained posterior samples for all models ranged between 0.500 and 0.501. Model 4 had the lowest DIC (4,795.7) followed by Model 3 (4,957.1), and Model 2 (8,523.5), while Model 1 had the highest DIC (8,926.6). However treating model parameters as fixed under models 2-4 resulted in large coefficients of variation suggesting that accounting for individual variability is important, with perhaps variability in L_∞ being more important based upon the low coefficient of variation in L_∞ from the base case of Model 1 and the large coefficients seen in Model 3 and Model 4 (Fig. 3).

3.3 Parameter estimation using maximum likelihood

The maximum likelihood approach used for Model 5 converged to produce estimates of μ_∞, σ_∞^2, K, $\mu_{\log A}$, σ_{logA}^2, and σ^2 (Table 5). Bootstrap confidence intervals of parameters μ_∞ and K overlapped L_∞ and K parameters from Bayesian models 1 and 2 (Table 1). From these results, it was concluded that estimates produced by maximum likelihood approaches were satisfactorily similar to estimates from the Bayesian approach. Model residuals appeared homoskedastic and normally distributed around zero for all but the largest fish. For fish with recapture lengths exceeding 60 cm, growth models underestimated observed recapture lengths (Fig. 4).

3.4 Comparing model performance

Across all 10,000 cross validation iterations used to determine the preffered integrated model structure, the six candidate models produced RMSE values that ranged between 2.78 and 4.95 (mean = 3.9, s.d. = 0.3), with lower values indicating a better fit to the data. The structure of

Model 11 outperformed competing models during cross validation (2,192 of 10,000 iterations). RMSE for this model ranged between 2.9 and 4.9 (mean = 3.9, s.d. = 0.3).

The inclusion of additional growth data improved the predictive capability of growth models compared to tagging data alone. Model 11 performed better than Model 5 during cross validation (5,672 of 10,000 iterations). Differences in RMSE between the competing structures of Models 11 and 5 ranged between -1.2 and 0.1 (mean = -0.1, s.d. = 0.1) with structure of Model 5, fit exclusively using tagging data, producing RMSE values that ranged between 2.8 and 5.3 (mean = 3.9, s.d. = 0.3). Bootstrapped parameter estimates refit using the structure of the prefered integrated model (Model 11) and the tagging only structure of Model 5 are summarized in Table 1 and all parameters for models 5-11 are reported in full in Table 5.

3.5 Sensitivity analysis

Parameters estimated using the observed and synthetic data differed by as much as 205.1% but were generally less than 21.3%. For all models, K differed more between the synthetic and observed data than L_∞. Across all models, when refit to the synthetic data, only Models 7 and 11 produced parameter estimates, that fell within the 95% confidence intervals estimated using the original OTP data. Model 7 was the most robust, with the smallest diffrence between L_∞ and K s estimated with real and synthetic datasets (1.13% and 8.7% respectively). The preferred integrated model (Model 11) was the second-best performing model overall with L_∞ differing by 2.45% and K by 15.47%. None of the point estimates for L_∞ and K estimated using the Bayesian models fit to the synthetic data fell within the 95% confidence intervals for the original models. Of the Bayesian models, parameter estimates for Model 1, the model which accounted for individual differences in each parameter and had the lowest coefficient of variation across both parameters, differed by 36.8% for the L_∞ and 122.5% for K when refit with the synthetic data. Parameters for Model 4, the Bayesian model with the lowest DIC score, differed between observed and synthetic data by 20.6% in the L_∞ and by 135.0% in K. Sensitivity results for all models are reported in full in Table 6.

4. Discussion

Our integrated model reconciles 30+ years of effort to quantify growth for *P. filamentosus* in the Hawaiian Archipelago and provide robust support for some previously estimated parameter values. Growth parameters derived using integrated models that incorporated additional length frequency and length-at-age data were better able to predict the growth observed in recaptured fish compared to those fit using only tagging data. These parameters were in agreement with direct aging studies where ages were estimated using 1) the fit of only integrated daily growth increments from otoliths collected in the NWHI without constraining L_∞ (Ralston and Miyamoto, 1983), 2) integrated daily growth increments and microincrement counts (DeMartini et al., 1994), and 3) the radioisotopic composition of otolith material and counts of otolith increments from the MHI and NWHI (Andrews et al., 2012) and support the implicit assumption that tagging individuals did not significantly disrupt their growth trajectory. integrated parameters differed from estimates from an ongoing mark recapture study in the MHI, which reported faster growth and smaller asymptotic lengths (O'Malley, 2015). These differences could arise from real changes in growth rate between the periods fish were collected, methodological differences in model interpretation, and/or that thus far, none of the fish recaptured during the ongoing study have been of the largest size classes (maximum size reported = 47.6 cm FL).

Compared to growth studies across their broader distribution, parameters obtained from the Hawaiian archipelago indicate that *P. filamentosus* were generally slower growing but obtained a larger asymptotic length than those from the Mariana Archipelago (Ralston and Williams, 1988) and Papua New Guinea (Fry et al., 2006; Andrews et al., 2012) and were faster growing but smaller in their asymptotic length when compared to estimates from the Seychelles (Hardman-Mountford et al., 1997; Mees, 1993; Mees and Rousseau, 1997; Pilling, 2000). These differences may represent genetic or phenotypic differences between these populations, or differences in the methods and sampling distribution between studies. It was not possible to distinguish between these two possibilities due to a lack of information on the gear used to sample and recapture fish in both these and the OTP study.

Of the Bayesian models, Model 1 was presumed optimal because it incorporated individual variability in both L_∞ and K. However, this model performed the worst of all Bayesian models during sensitivity analysis. Models 2-4 suggest that individual variability in both K and L_∞ s is important, with perhaps variability in L_∞ being more important based on the similar parameter estimates obtained from Models 1 and 2 and comparison of relatively small the coefficient of variation for L_∞ from the base case of Model 1 to the larger coefficients of variation under assumptions of constrained individual variability in Model 3 and Model 4 (Fig. 3). Based on these parameter estimates and pattern of large standard deviations, it is likely Models 3 and 4 were not credible despite lower DIC values and performing well during sensitivity analysis. Similar parameter estimates obtained from Models 1 and 2 suggested that the primary source of individual variability was due to variability in the L_{∞} parameter. This is consistent with other studies where the best models accounted for individual variability in both terms but accounting for individual variation in the L_{∞} term alone was sufficient to describe growth while significantly reducing computational complexity (Eveson et al., 2007; Zhang et al., 2009). However, during the sensitivity analysis all of the Bayesian models failed to produce parameter estimates that fell within the 95% confidence intervals estimated from the original data, suggesting sensitivity in the estimated parameters to the sampling distribution of fish across size classes.

The treatement of individual variability in parameters for Model 2 were identical to those used to fit Model 5 (OTP data only). Comparing growth parameter estimates from these models indicate that Bayesian and maximum likelihood fitting methods performed similarly. Parameter estimates for Models 1 and 2 were contained within the 95% confidence intervals of Model 5. These results suggest that treatment of K as a fixed effect was unlikely to bias estimates in integrated models, fit using maximum likelihood, which were evaluated under the same assumptions as models 2 and 5.

Of all models presented, Model 11 was the best performing during predictive during cross validation and was one of only two models that proved robust to the sensitivity analysis. While information from older/larger fish from direct aging datasets was very important for grounding the upper end of integrated growth curves and resulted in parameters that better predicted length at recapture, these additional data sources were less influential to the best performing models than for those otherwise identical in structure but placing a greater emphasis on those additional data sources. This result suggests that the inclusion of additional data was important for obtaining accurate results but were most helpful when their influence was limited.

The additional sources of data included here represent collections spanning several decades from the MHI and NWHI. When incorporating these additional data sources, it is an inherent assumption that growth within the population did not differ significantly with time or region. This is not the first study to make these assumptions; with the exception of Ralston and Miyamoto (1983), all subsequent studies of growth for *P. filamentosus* in the Hawaiian archipelago have included datasets or parameter estimates from one or more previous studies in their calculations without regard to the time and place the data was collected (DeMartini et al., 1994; Moffitt and Parrish, 1996; Andrews et al., 2012). Genetic homogeneity between NWHI and MHI stocks provides some justification for pooling data across regions. However, these spatial and temporal assumptions may not reflect phenotypic realities and further work is required to resolve whether differences in growth exist between the two regions (Gaither et al. 2010, 2011).

Sexual size dimorphism may explain the tendency of parameters obtained here and elsewhere to underestimate the length at recapture observed for the largest fish in the OTP dataset (approximate fork length > 50 cm) (Fig. 4). For sex agnostic models, parameters are essentially averaged between sexes. In smaller sizes classes where the sex ratio of individuals is similar to that of the total population, this averaging of parameters between sexes results in increased estimates of variance. However, if dimorphic differences in growth are present and one sex disproportionately attains a greater asymptotic length than the other, that sex is likely to be overrepresented in the largest size classes relative to the total population. Growth estimated for these individuals continues to represent an average of both sexes and will result in the underestimation of lengths at recapture, while growth in the underrepresented sex will be overestimated. This produces a residual pattern resembling the one seen in the OTP data.

While not pronounced, dimorphic size differences have been observed in a number of lutjanid species (Grimes, 1987; Mees, 1993; Newman et al., 2000; Newman and Dunk, 2002; Nichols, 2019; Taylor et al., 2018; Williams et al., 2017). Elsewhere in their distribution, larger asymptotic lengths have been reported for male *P. filamentosus* in the Seychelles, research fishing in the Northwestern Hawaiian Islands found, the number of females outnumbered males almost 2:1 in the largest size classes, and in Guam no differences between sexes were observed (Kami, 1973; Kikkawa, 1984; Mees, 1993). Estimation of growth parameters for *P. filamentosus* in the Central Pacific have thus far remained sex agnostic and a method for non-invasive sexing of this species was unknown until recently (Luers et al., 2017). Therefore, these differences may reflect true sexual dimorphism or discrepancies between the structure of the sampled and true populations. More work addressing sex specific differences is required to adequately test for dimorphism in this region.

Accurate estimates of von Bertalanffy growth parameters are very important for management. Growth parameters are often used directly or indirectly in stock assessment and fisheries management (Haight et al., 1993; Polovina et al., 1987). These efforts are sensitive to both growth parameters and the model used to estimate those parameters. For example, the rate of instantaneous natural mortality *M* is a value of interest often inferred from *K* using empirical relationships (Jensen, 1996; Ralston, 1987; Thorson et al., 2017). Underestimating *K* will underestimate *M*, characterizing a stock as less productive than it actually is while overestimating *K* will have the opposite effect. If a management regime is linked to such a flawed estimate of stock productivity, then the stock is likely to be mismanaged and under or over harvested, respectively, relative to its true biological potential. Future work to refine these estimates for *P. filamentosus* should consider how the distribution of the sampled population and dimorphic differences between males and females may affect their respective life histories.

Acknowledgements

The authors would like to thank everyone involved with OTP. We are also thankful to the authors of the other studies that collected the data presented here including Frank Parrish, Robert Moffitt, Stephen Ralston, Garret Miyamoto, Allen Andrews, Edward DeMartini, Jon Brodziak, Ryan Nichols, and Robert Humphreys. Thanks to Annette Tagawa for providing the OTP mark recapture data used in this analysis. We would also like to thank Zane Zhang and Paige Eveson for providing code used to fit Bayesian and maximum likelihood models. Finally, we would like to thank Joe O'Malley and Frank Parrish for their advice and feedback during this project and Allen Andrews for reviewing our manuscript. Funding for this project was provided by the State of Hawaii's Department of Land and Natural Resources (DLNR) under awards F12A01319, F13AF00667, and F14AF00514, from the Sport Fish Restoration Program administered by the US Fish and Wildlife Service (to KCW) and NOAA award #NA10NMF4520163 (to ECF). This is SOEST contribution ###### and HIMB contribution ####.

Competing Interests

The authors declare that they have no competing interests.

References

Allen, G.R., 1985. Fao Species Catalogue Vol . 6 . Snappers of the World. Fao Fish. Synopsis 6, 208. https://doi.org/10.1016/0025-326X(92)90600-B

Andrews, A.H., DeMartini, E.E., Brodziak, J., Nichols, R.S., Humphreys, R.L., 2012. A long-lived life history for a tropical, deepwater snapper (Pristipomoides filamentosus): bomb radiocarbon and lead-radium dating as extensions of daily increment analyses in otoliths. Can. J. Fish. Aquat. Sci. 69, 1850–1869. https://doi.org/10.1139/f2012-109

Benaglia, T., Chauveau, D., Hunter, D.R., Young, D., 2009. Mixtools: An R package for

analyzing finite mixture models. J. Stat. Softw. 32, 1–29.
Bolser, D. G., Grüss, A., Lopez, M. A., Reed, E. M., Mascareñas-Osorio, I., & Erisman, B. E. (2018). The influence of sample distribution on growth model output for a highly-exploited marine fish, the Gulf Corvina (Cynoscion othonopterus). PeerJ, 6, e5582.
Burman, P., 1989. A comparative study of ordinary cross-validation, v-fold cross-validation and the repeated learning-testing methods. Biometrika 76, 503–514. https://doi.org/10.1093/biomet/76.3.503
Cailliet, G. M., & Tanaka, S. (1990). Recommendations for research needed to better understand the age and growth of elasmobranchs. Elasmobranchs as Living Resources: Advances in the Biology, Ecology, Systematics, and the Status of the Fisheries, WS Pratt, Jr., SH Gruber, and T. Taniuchi, Eds., NOAA Tech. Rep, 90, 505-507.
DeMartini, E.E., Landgraf, K.C., Ralston, S., 1994. A recharacterizatinon of the age-length and growth relationships of Hawaiian snapper Pristipomoides filamentosus. U.S. Department of Commerce, National Oceanic and Atmospheric Administration, National Marine Fisheries Service, Southwest Fisheries Science Center, Honolulu, HI.
Eveson, J.P., Laslett, G.M., Polacheck, T., 2004. An integrated model for growth incorporating tag–recapture, length–frequency, and direct aging data. Can. J. Fish. Aquat. Sci. 61, 292–306. https://doi.org/10.1139/f03-163
Eveson, J.P., Polacheck, T., Laslett, G.M., 2007. Consequences of assuming an incorrect error structure in von Bertalanffy growth models: a simulation study. Can. J. Fish. Aquat. Sci. 64, 602–617. https://doi.org/10.1139/f07-036
Fabens, A.J., 1965. Properties and fitting of the von Bertalanffy growth curve. Growth 29, 265–289.
Francis, R. I. C. C., 1988a. Are Growth Parameters Estimated from Tagging and Age–Length Data Comparable? Can. J. Fish. Aquat. Sci. 45, 936–942. https://doi.org/10.1139/f88-115
Francis, R. I.C.C., 1988b. Maximum likelihood estimation of growth and growth variability from tagging data. New Zeal. J. Mar. Freshw. Res. 22, 43–51. https://doi.org/10.1080/00288330.1988.9516276
Fry, G.C., Brewer, D.T., Venables, W.N., 2006. Vulnerability of deepwater demersal fishes to commercial fishing: Evidence from a study around a tropical volcanic seamount in Papua New Guinea. Fish. Res. 81, 126–141. https://doi.org/10.1016/j.fishres.2006.08.002
Gaither, M.R., Toonen, R.J., Sorenson, L., Bowen, B.W., 2010. Isolation and characterization of microsatellite markers for the crimson jobfish, pristipomoides filamentosus (Lutjanidae). Conserv. Genet. Resour. 2, 169–172. https://doi.org/10.1007/s12686-009-9119-3
Gaither, M.R., Jones, S. a., Kelley, C., Newman, S.J., Sorenson, L., Bowen, B.W., 2011. High connectivity in the deepwater snapper Pristipomoides filamentosus (lutjanidae) across the indo-pacific with isolation of the Hawaiian archipelago. PLoS One 6, 1–13. https://doi.org/10.1371/journal.pone.0028913
Gelman, A., Rubin, D.B., 1992. lnference from iterative simulation using multiple sequences. Stat. Sci. 7, 457–472. https://doi.org/10.2307/2246093
Goodyear, C.P., 2019. Modeling Growth: Consequences from Selecting Samples by Size. Trans. Am. Fish. Soc. 148, 528–551. https://doi.org/10.1002/tafs.10152
Grimes, C.B., 1987. Reproductive biology of the Lutjanidae: A review, in: Polovina, J.J., Ralston, S. (Eds.), Tropical Snappers and Groupers: Biology and Fisheries Management. Westview Press, Boulder, Colorado, pp. 239–294.
Haight, W.R., Kobayashi, D.R., Kawamoto, K.E., 1993. Biology and management of deepwater

snappers of the Hawaiian archipelago. Mar. Fish. Rev. 55, 20–27.
Hardman-Mountford, N.J., Polunin, N.V.C., Boulle, D., 1997. Can the age of the tropical species be determined by otolith measurement?: a study using Pristipomoides filamentosus (Pisces: Lutjanidae) from the Mahe Plateau, Seychelles. Naga, ICLARM Q. 20, 27–31.
Hawaii Reported Landing Tables [WWW Document], 2016. URL https://www.pifsc.noaa.gov/wpacfin/hi/dar/Pages/hi_data_3.php (accessed 3.23.18).
James, I.R., 1991. Estimation of von Bertalanffy growth curve parameters from recapture data. Biometrics 47, 1519–1530. https://doi.org/10.2307/2532403
Jensen, A.L., 1996. Beverton and Holt life history invariants result from optimal trade-off of reproduction and survival. Can. J. Fish. Aquat. Sci. 53, 820–822. https://doi.org/10.1139/f95-233
Kami, H.T., 1973. The Pristipomoides (Pices: lutjanidae) of Guam with notes on their biology. Micronesica 9, 97–117. https://doi.org/10.1080/15235882.2014.934485
Kapur, M., Haltuch, M., Connors, B., Rogers, L., Berger, A., Koontz, E., Cope, J., Echave, K., Fenske, K., Hanselman, D., Punt, A.E., 2020. Oceanographic features delineate growth zonation in Northeast Pacific sablefish. Fish. Res. 222. https://doi.org/10.1016/j.fishres.2019.105414
Kikkawa, B.S., 1984. Maturation, spawning, and fecundity of Opakapaka, Pristipomoides filamentosus, in the Northwest Hawaiian Islands. Proc. Second Symp. Resour. Investig. Northwest. Hawaiian Islands.
Kimura, D.K., Shimada, A.M., Lowe, S.A., 1993. Estimating von Bertalanffy growth parameters of sablefish Anoplopoma fimbria and Pacific cod Gadus macrocephalus using tag-recapture data. Fish. Bull. 91, 271–280.
Kobayashi, D.R., 2008. Spatial connectivity of Pacific insular species: insights from modeling and tagging. Ph.D. thesis, 215p. University of Technology. Sydney, Australia.
Langseth, B., Syslo, J., Yau, A., Kapur, M., Brodziak, J., 2018. Stock assessment for the main Hawaiian Islands Deep 7 bottomfish complex in 2018, with catch projections through 2022. NOAA Tech. Memo. NMFS-PIFSC 69, 217.
Laslett, G.M., Eveson, J.P., Polacheck, T., 2002. A flexible maximum likelihood approach for fitting growth curves to tag-recapture data. Can. J. Fish. Aquat. Sci. 59, 976–986. https://doi.org/10.1139/f02-069
Laslett, G.M., Eveson, J.P., Polacheck, T., 2004. Fitting growth models to length frequency data. ICES J. Mar. Sci. 61, 218–230. https://doi.org/10.1016/j.icesjms.2003.12.006
Luers, M.A., DeMartini, E.E., Humphreys, R.L.J., 2017. Seasonality, sex ratio, spawning frequency and sexual maturity of the opakapaka Pristipomoides filamentosus (Perciformes: Lutjanidae) from the Main Hawaiian Islands: fundamental input to size-at-retention regulations. Mar. Freshw. Res. 69, 325–335. https://doi.org/10.1071/MF17195
Maller, R.A., Deboer, E.S., 1988. An analysis of two methods of fitting the von Bertalanffy curve to capture-recapture data. Mar. Freshw. Res. 39, 459–466. https://doi.org/10.1071/MF9880459
Maunder, M.N., Crone, P.R., Valero, J.L., Semmens, B.X. (Eds.), 2015. Growth: theory, estimation, and application in fishery stock assessment, in: CAPAM Workshop Series Report 2. Center for the Advancement of Population Assessment Methodology, La Jolla, CA, p. 55.
Mees, C.C., 1993. Population biology and stock assessment of Pristipomoides filamentosus on the Mahe Plateau, Seychelles. J. Fish Biol. 43, 695–708. https://doi.org/10.1111/j.1095-

8649.1993.tb01147.x
Mees, C.C., Rousseau, J.A., 1997. The potential yield of the lutjanid fish Pristipomoides filamentosus from the Mahe Plateau, Seychelles: Managing with uncertainty. Fish. Res. 33, 73–87. https://doi.org/10.1016/S0165-7836(97)00069-6
Meng, X.-L., 1994. Posterior predictive p-values. Ann. Stat. 22, 1142–1160.
Moffitt, R.B., Parrish, F. a, 1996. Habitat and life history of juvenile Hawaiian pink snapper, Pristipomoides filamentosus. Pacific Sci. 50, 371–381.
Newman, S.J., Cappo, M., Williams, D.M.B., 2000. Age, growth and mortality of the stripey, Lutjanus carponotatus (Richardson) and the brown-stripe snapper, L. vitta (Quoy and Gaimard) from the central Great Barrier Reef, Australia. Fish. Res. 48, 263–275. https://doi.org/10.1016/S0165-7836(00)00184-3
Newman, S.J., Dunk, I.J., 2002. Growth, age validation, mortality, and other population characteristics of the red emperor snapper, Lutjanus sebae (Cuvier, 1828), off the Kimberley coast of north-western Australia. Estuar. Coast. Shelf Sci. 55, 67–80. https://doi.org/10.1006/ecss.2001.0887
Nichols, R.S., 2019. Sex-specific growth and longevity of "Ehu", Etelis carbunculus (Family lutjanidae) within the Hawaiian archipelago. University of Hawaii.
Okamoto, H.M., 1993. Final report of the Hawaii Department of Land and Natural Resources to the National Oceanic and Atmospheric Administration Pursuant to NOAA Award No. NA90AA-D-IJ466. Hawaii Department of Land and Natural Resources. Honolulu, HI. 7p + appendicies
O'Malley, J., 2015. A Review of the Cooperative Hawaiian Bottomfish Tagging Program of the Pacific Islands Fisheries Science Center and the Pacific Islands Fisheries Group. Honolulu, HI. https://doi.org/10.7289/V59W0CF7
Oyafuso, Z.S., Drazen, J.C., Moore, C. H., Franklin, E. C. 2018. Habitat-based species distribution modelling of the Hawaiian deepwater snapper-grouper complex. Fisheries Research 195: 19-27. https://doi.org/10.1016/j.fishres.2017.06.011
Palmer, M.J., Phillips, B.F., Smith, G.T., 1991. Application of nonlinear models with random coefficients to growth data. Biometrics 47, 623–635. https://doi.org/10.2307/2532151
Pilling, G.M., 2000. Validation of annual growth increments in the otoliths of the lethrinid Lethrinus mahsena and the lutjanid Aprion virescens from sites in the tropical Indian Ocean, with notes on the nature of growth increments in Pristipomoides filamentosus. Fish. Bull. 98, 600–611.
Plummer, M., 2003. JAGS: A program for analysis of Bayesian graphical models using Gibbs sampling. In Proceedings of the 3rd international workshop on distributed statistical computing, in: Proceedings of the 3rd International Workshop on Distributed Statistical Computing. Vol. 124.
Polovina, J.J., Ralston, S., Ralston, S., 1987. Assessment and management of deepwater bottom fishes in Hawaii and the Marianas. Trop. snappers groupers Biol. Fish. Manag. 505–532.
R Core Team, 2014. R: A Language and Environment for Statistical Computing.
Radtke, R.L., 1987. Age and growth information available from the otoliths of the Hawaiian snapper, Pristipomoides filamentosus. Coral Reefs 6, 19–25. https://doi.org/10.1007/BF00302208
Ralston, S., Miyamoto, G.T., 1983. Analyzing the width of daily otolith increments to age the Hawaiian snapper, Pristipomoides filamentosus. Fish. Bull. 81, 523–535.
Ralston, S.V.D., 1987. Mortality rates of snappers and groupers. Trop. snappers groupers Biol.

Fish. Manag. 375–404.
Ralston, S.V.D., Polovina, J., 1982. A multispecies analyis of the commercial deep-sea handline fishery in Hawaii. Fish. Bull. 80, 435–448.
Ralston, S.V., 1988. Depth distributions, growth, and mortality of deep slope fishes from the Mariana Archipelago. NOAA Tech. Memo. NMFS-SWFC 113, 143.
Sainsbury, K.J., 1980. Effect of individual variability on the von Bertalanffy growth equation. Can. J. Fish. Aquat. Sci. 37, 241–247. https://doi.org/10.1139/f80-031
Su, Y., Yajima, M., 2012. R2jags: A Package for Running JAGS from R.
Tanaka, S., Cailliet, G.M., Yudin, K.G., 1990. Differences in Growth of the Blue Shark, Prionace glauca: Technique or population? Biology (Basel). 177–187.
Taylor, B.M., Oyafuso, Z.S., Pardee, C.B., Ochavillo, D., Newman, S.J., 2018. Comparative demography of commercially-harvested snappers and an emperor from American Samoa. PeerJ 6, e5069. https://doi.org/10.7717/peerj.5069
Thorson, J.T., Munch, S.B., Cope, J.M., Gao, J., 2017. Predicting life history parameters for all fishes worldwide. Ecol. Appl. 27, 2262–2276. https://doi.org/10.1002/eap.1606
Uchiyama, J.H., Tagami, D.T., 1984. Life history, distribution, and abundance of bottomfishes in the Northwestern Hawaiian Islands, in: Grigg, R.W., Tanoue, K.Y. (Eds.), Proceedings of the Second Symposium on Resource Investigations in the Northwestern Hawaiian Islands. pp. 229–247.
Wakefield, C.B., O'Malley, J.M., Williams, A.J., Taylor, B.M., Nichols, R.S., Halafihi, T., Humphreys, R.L., Kaltavara, J., Nicol, S.J., Newman, S.J., 2017. Ageing bias and precision for deep-water snappers: Evaluating nascent otolith preparation methods using novel multivariate comparisons among readers and growth parameter estimates. ICES J. Mar. Sci. 74, 193–203. https://doi.org/10.1093/icesjms/fsw162
Wang, Y.-G., Thomas, M.R., Somers, I.F., 1995. A maximum likelihood approach for estimating growth from tag–recapture data. Can. J. Fish. Aquat. Sci. 52, 252–259. https://doi.org/10.1139/f95-025
Williams, A.J., Wakefield, C.B., Newman, S.J., Vourey, E., Abascal, F.J., Halafihi, T., Kaltavara, J., Nicol, S.J., 2017. Oceanic, Latitudinal, and Sex-Specific Variation in Demography of a Tropical Deepwater Snapper across the Indo-Pacific Region. Front. Mar. Sci. 4. https://doi.org/10.3389/fmars.2017.00382
Zhang, Z., Lessard, J., Campbell, A., 2009. Use of Bayesian hierarchical models to estimate northern abalone, Haliotis kamtschatkana, growth parameters from tag-recapture data. Fish. Res. 95, 289–295. https://doi.org/10.1016/j.fishres.2008.09.035

Tables

Table 1. Estimates (and 95% confidence intervals when available) of von Bertalanffy growth parameters L_∞, K, and t_o reported by the present and prior studies.

Table 2. Summary of tagging and recapture locations for *P. filamentosus* used for growth increment approaches as referenced to reporting grids in Figure 1. Adapted from Kobayashi (2008).

Table 3. Von Bertalanffy growth parameter estimates from Bayesian hierarchical growth models (Models 1-4).

Table 4. A reference for the candidate model structures used to determine the preferred model structure from integrated maximum likelihood growth models (Models 5-11).

Table 5. Sample and Population Parameter Estimates (with bootstrapped confidence intervals) from Maximum Likelihood Growth Models (Models 5-11).

Table 6. Parameter estimates obtained from a sensitivity analysis where tagging data was divided into 5 cm bins and then synthetic data was added so that each bin contained 200 observations. Comparing parameter estimates fit to synthetic data against those from the original dataset provide a metric to compare the effect of the sampling distribution on the estimates obtained.

Figure Captions

Figure 1. Reporting Grid Map.

Map showing the location and number of the State of Hawaii's statistical reporting grids corresponding to the reported location of tagging and recaptured for fish summarized in Table 5.2.

Figure 2. Length and Time at Liberty for OTP and Additional Data.

The length of P. filamentosus recaptured and included in analysis of OTP tagging data and the distribution of times at liberty are presented in subplots a and b respectively. The fork length of fish during tagging is highlighted in blue while length at recapture is shown in red. Subplot c shows the measured fork length and estimated ages from the various sources of length at age data included in models 6 – 10 while subplot d tracks the mode fork length for cohorts included in the length frequency data originally presented by Moffitt and Parrish (1996), also used to supplement OTP data in models 6-10.

Figure 3. Coefficient of Variation for von Bertalanffy Growth Function Parameters.

Coefficient of variation for 2 von Bertalanffy growth function parameters (Brody growth coefficient, K and mean asymptotic length, $L\infty$) for P. filamentosus. Individual variability was examined incorporating individual variability in both parameters, in either one of the parameters in series, or in neither parameter.

Figure 4. Plots Comparing Predicted and Observed Length at Recapture.

Predicted lengths at recapture compared to the observed lengths at recapture for tagged P. filamentosus. Length at recapture was predicted as a function of length at marking, time at liberty, and parameter point estimates. The 1:1 line indicates where points would fall if model parameters perfectly predicted length at recapture.

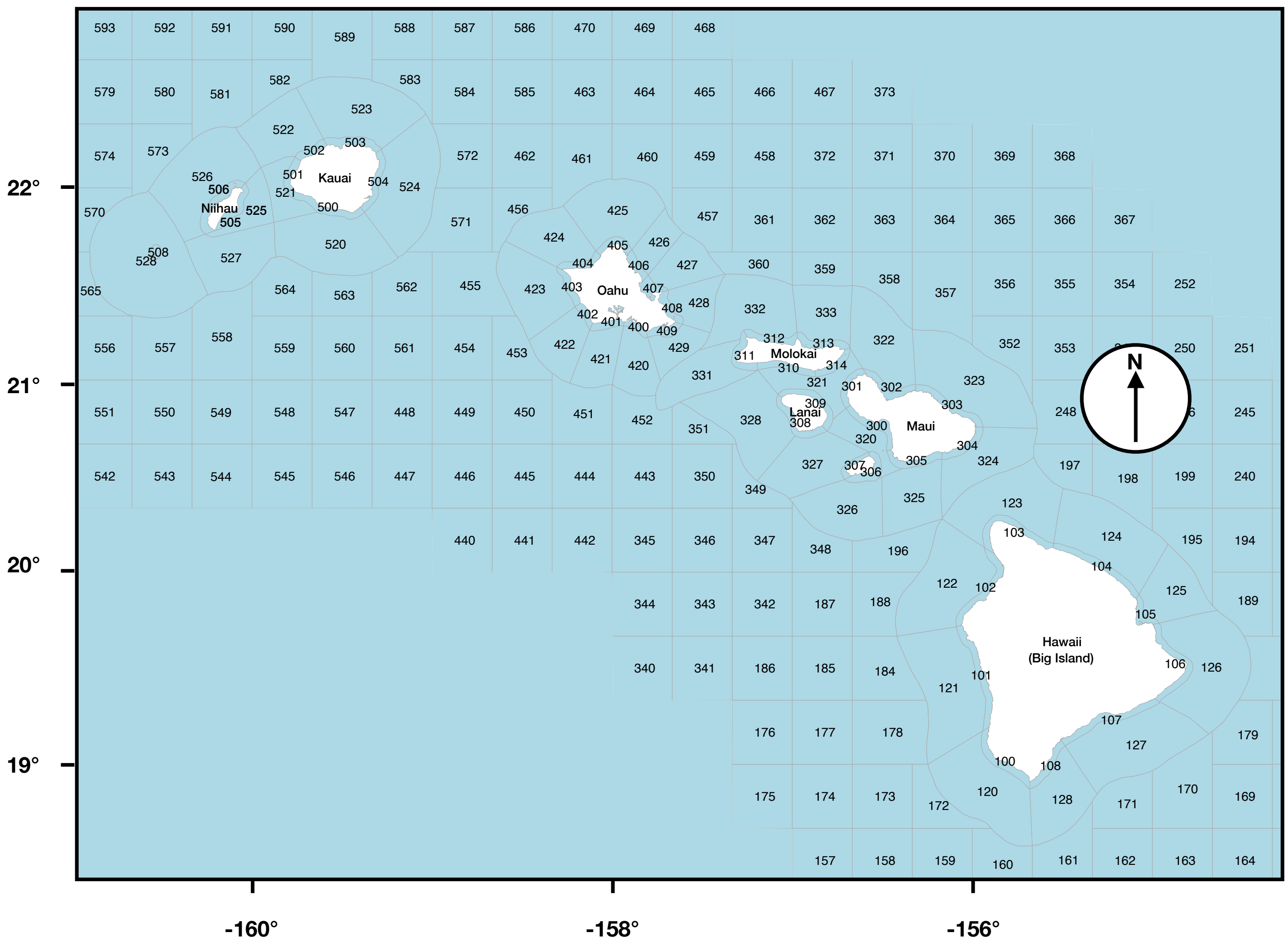
593
592
591
590
589
588
587
586
470
469
468
579
580
581
582
583
584
585
463
464
465
466
467
373
523
574
573
522
502
503
572
462
461
460
459
458
372
371
370
369
368
526
506
501
Kauai
504
524
521
570
Niihau
525
505
500
571
456
425
457
361
362
363
364
365
366
367
424
426
508
528
527
520
405
406
427
360
359
358
357
356
355
354
252
404
403
Oahu
407
565
564
563
562
455
423
408
428
332
333
402
401
400
409
558
312
313
322
352
353
250
251
556
557
559
560
561
454
453
422
429
311
Molokai
310
314
421
420
331
321
301
302
323
551
550
549
548
547
448
449
450
451
452
309
Lanai
308
328
351
303
248
245
300
Maui
320
304
542
543
544
545
546
447
446
445
444
443
350
327
307
306
305
324
197
198
199
240
349
325
326
123
440
441
442
345
346
347
348
196
103
124
195
194
104
122
102
125
344
343
342
187
188
189
105
Hawaii
(Big Island)
340
341
186
185
184
106
126
121
101
107
176
177
178
179
127
100
108
120
175
174
173
172
128
171
170
169
157
158
159
160
161
162
163
164
N
22°
21°
20°
19°
-160°
-158°
-156°

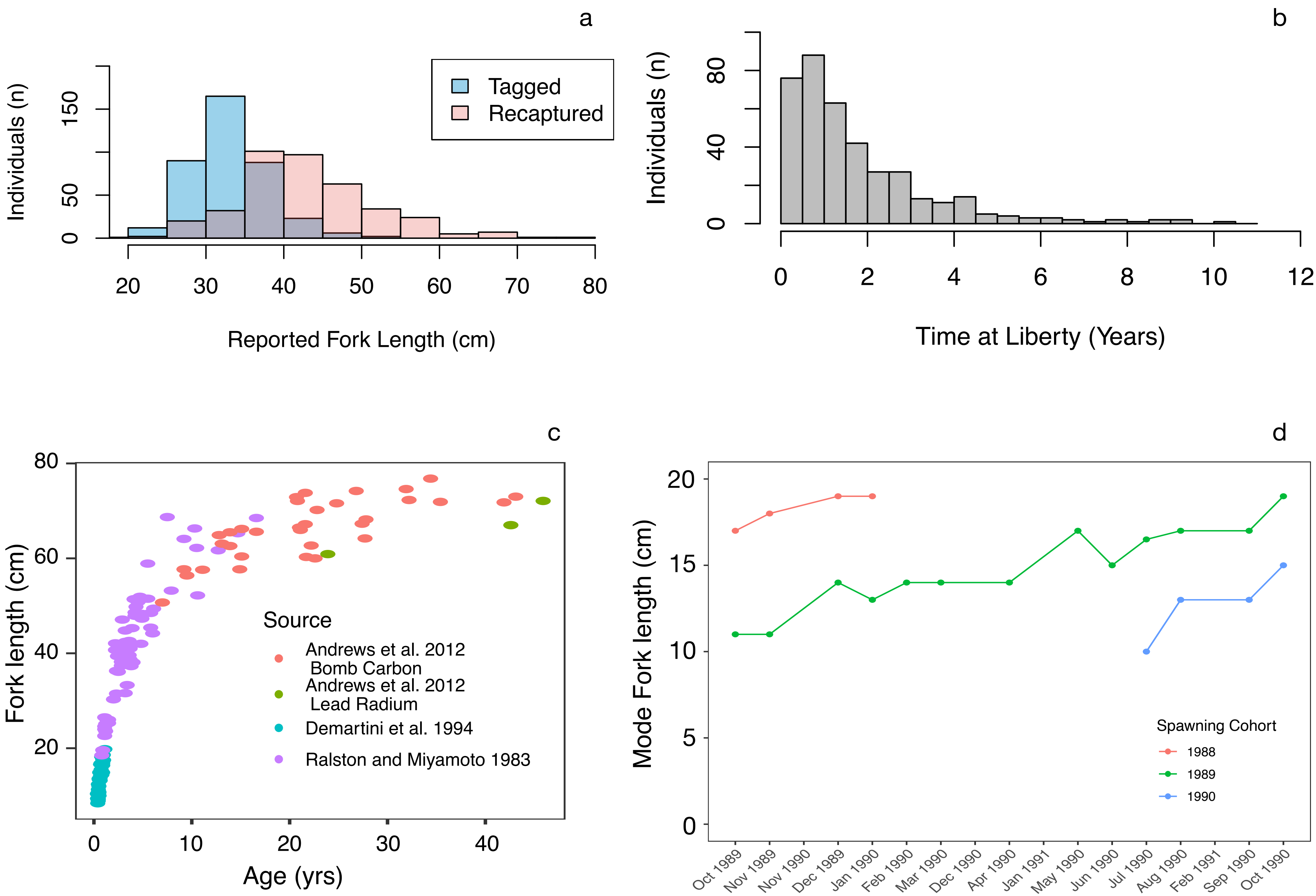

a
Tagged
Recaptured
Individuals (n)
0
50
150
20
30
40
50
60
70
80
Reported Fork Length (cm)
b
Individuals (n)
0
40
80
0
2
4
6
8
10
12
Time at Liberty (Years)
c
Fork length (cm)
20
40
60
80
0
10
20
30
40
Age (yrs)
Source
Andrews et al. 2012 Bomb Carbon
Andrews et al. 2012 Lead Radium
Demartini et al. 1994
Ralston and Miyamoto 1983
d
Mode Fork length (cm)
0
5
10
15
20
Oct 1989
Nov 1989
Nov 1990
Dec 1989
Jan 1990
Feb 1990
Mar 1990
Dec 1990
Apr 1990
Jan 1991
May 1990
Jun 1990
Jul 1990
Aug 1990
Feb 1991
Sep 1990
Oct 1990
Spawning Cohort
1988
1989
1990

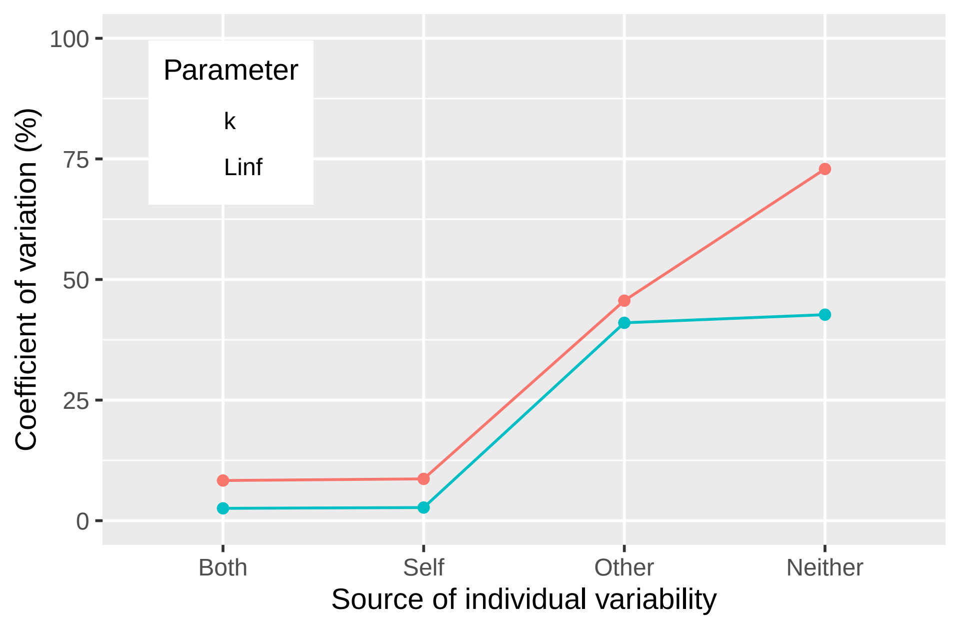
Parameter
k
Linf
100
75
50
25
0
Coefficient of variation (%)
Both
Self
Other
Neither
Source of individual variability

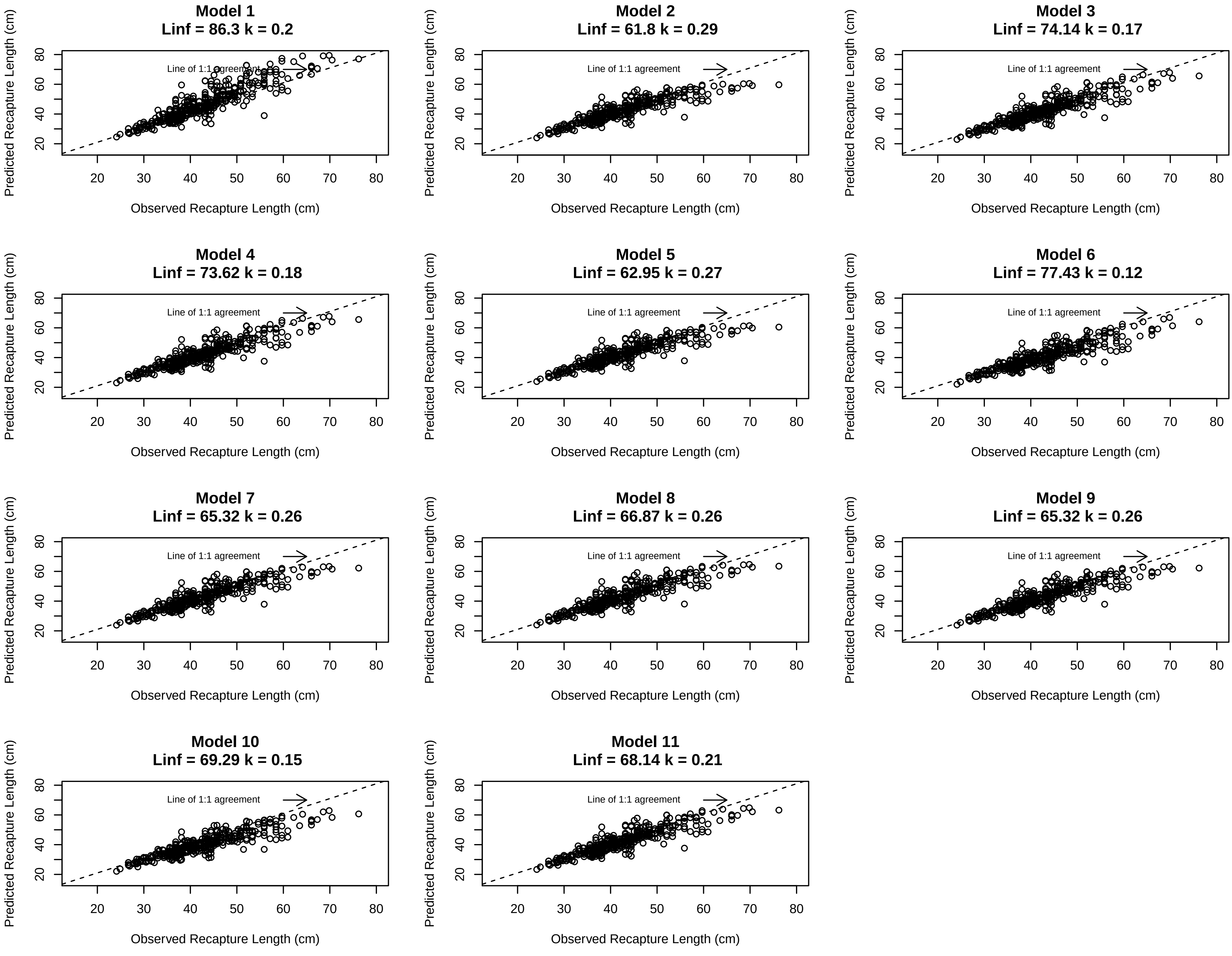
Model 1
Linf = 86.3 k = 0.2
Model 2
Linf = 61.8 k = 0.29
Model 3
Linf = 74.14 k = 0.17
Model 4
Linf = 73.62 k = 0.18
Model 5
Linf = 62.95 k = 0.27
Model 6
Linf = 77.43 k = 0.12
Model 7
Linf = 65.32 k = 0.26
Model 8
Linf = 66.87 k = 0.26
Model 9
Linf = 65.32 k = 0.26
Model 10
Linf = 69.29 k = 0.15
Model 11
Linf = 68.14 k = 0.21
Line of 1:1 agreement
Predicted Recapture Length (cm)
Observed Recapture Length (cm)
20
30
40
50
60
70
80

	Method	Region	Otolith Growth Bands	Otoliths (Bomb-Carbon)	Pooled Otoliths (Lead-Radium)	Monthly Length Frequency	Recaptured Fish	Linf (95% CI)	K (95% CI)	to (95% CI)	Source
Direct Aging	Daily Increments	NWHI	17	-	-	-	-	-	-	-	Moffitt (1980)
	Daily Increments	NWHI	N.R.	-	-	-	-	80.5	0.16	-	Ralston (1980)
	Daily Growth Integration	NWHI	64	-	-	-	-	78	0.146	-1.67	Ralston & Miyamoto (1983)*
	Daily Growth Integration	NWHI	64	-	-	-	-	66.4	0.235	-0.81	Ralston & Miyamoto (1983)
	Daily Increments & Integration	NWHI	N.R.	-	-	-	-	69.8	0.534	0.18	Radtke (1987)
	Daily Increments & Integration	MHI & NWHI	92	-	-	-	-	70.4 (63.9 - 76.9)	0.25 (0.20, 0.31)	-0.22 (-0.39, -0.06)	DeMartini et al. (1994)
	Annual Increments	NWHI	N.R.	-	-	-	-	97.1	0.31	0.02	Uchiyama & Tagami (1984)
	Daily Increments, Integration, & Radioisotopes	MHI & NWHI	100	33	3	-	-	67.5 (65.7, 69.3)	0.242 (0.185, 0.299)	-0.29 (-0.38, -0.20)	Andrews et. al (2012)
	Modal Progression	MHI	-		-	13		78	0.21	0	Moffit & Parrish (1996)*
Growth Increment	Mark Recapture	MHI	-		-	-	96	71.55	0.15	-	O'Malley (2015) - Gulland and Holt
	Mark Recapture	MHI	-		-	-	96	57.80 (55.97, 58.67)	0.28 (0.25, 0.31)	-	O'Malley (2015) - Francis
	Mark Recapture	MHI	-		-	-	387	61.41 (58.08 - 65.24)	0.29 (0.24 - 0.35)	-	Present Study - Bayesian Model 1
	Mark Recapture	MHI	-		-	-	387	73.68 (61.87 - 83.54)	0.18 (0.13 - 0.23)	-	Present Study - Bayesian Model 4
	Mark Recapture	MHI	-		-	-	387	62.95 (56.17, 66.67)	0.30 (0.23, 0.39)	-	Present Study - Maximum Likelihood Model 5
	Integrative	MHI & NWHI	113	33	3	13	378	68.14 (65.42, 69.54)	0.22 (0.20, 0.25)	-0.37 (-0.47, -0.28)	Present Study - Integrative Model 11

* Linf parameter constrained during fit

RELEASE LOCATION

TAGGING LOCATION	127	304	306	307	308	309	311	312	313	320	321	327	331	332	351	401	402	403	404	405	407	408	409	421	423	424	428	429	452	505	528	Total
127							1																									1
304				1						2																						3
306			1							1																						2
307				5								1																				6
308			1		2						5																					8
309											2																					2
311							25	1					4																			30
312							1	1																								2
313				1				1					3																			5
320			1	3						24		1																				29
321											31																					31
327				3						2		2																				7
331							46	2					128			4																180
332													1																			1
351													1																			1
401																131																131
402																1																1
403																1																1
404																						1										1
405							1															1										2
407													1									12										13
408													1																			1
409																4								1								5
421																14						1										15
423											1					14						1										16
424					1								4			3						3										11
428							2	1					2																			5
429							2				1		1			1																5
452											1		1																			2
505										1																						1
528							2																									2
No Recovery	1	3	44	278	35	2	582	168	5	333	429	84	875	1	1	937	7	1	1	2	2	293	4	20	16	9	8	5	2	1	2	4151
Total	1	3	47	291	38	2	662	174	5	363	470	88	1022	1	1	1110	7	1	1	2	2	312	4	21	16	9	8	5	2	1	2	4671

	Parameter	Mean	SD	2.50%	Median	97.50%	Rhat	n eff
Model 1	Linf_mu	61.41	1.83	58.09	61.31	65.24	1.00	1600
	Linf_std	5.29	0.35	4.61	5.29	5.99	1.00	26000
	Linf_tau	0.04	0.00	0.03	0.04	0.05	1.00	26000
	Shape	31.14	5.35	22.39	30.56	43.45	1.00	2500
	deviance	3404.45	105.13	3185.37	3408.41	3597.48	1.00	2400
	k_mu	0.29	0.03	0.24	0.29	0.35	1.00	1400
	k_std	0.01	0.00	0.00	0.01	0.02	1.00	6300
	k_tau	16745.57	11200.94	3500.58	13971.34	45707.55	1.00	6300
	rate	11.70	1.82	8.69	11.51	15.84	1.00	4200
	tau	0.21	0.03	0.16	0.21	0.28	1.00	3300
	variance	4.81	0.69	3.54	4.78	6.23	1.00	3300
Model 2	Linf_mu	61.79	1.80	58.52	61.69	65.62	1.00	1300
	Linf_std	5.33	0.35	4.65	5.32	6.02	1.00	64000
	Linf_tau	0.04	0.00	0.03	0.04	0.05	1.00	64000
	Shape	31.11	5.09	22.68	30.59	42.69	1.00	3100
	deviance	3413.19	101.12	3201.74	3417.04	3599.66	1.00	4300
	k_mu	0.29	0.03	0.23	0.29	0.35	1.00	2000
	k_std	0.02	0.02	0.01	0.01	0.05	1.00	110000
	k_tau	10173.40	10098.44	341.07	7109.57	37300.82	1.00	110000
	rate	11.57	1.75	8.66	11.39	15.53	1.00	5400
	tau	0.21	0.03	0.16	0.21	0.28	1.00	4900
	variance	4.86	0.68	3.61	4.84	6.26	1.00	4900
Model 3	Linf_mu	73.69	4.96	61.78	73.78	83.30	1.00	17000
	Linf_std	22.02	2002.46	0.01	0.50	61.48	1.00	50000
	Linf_tau	717.79	2585.99	0.00	3.97	7484.98	1.00	50000
	Shape	63.54	13.65	41.43	61.85	93.77	1.01	300
	deviance	3848.01	47.10	3757.62	3847.50	3941.99	1.00	9300
	k_mu	0.17	0.01	0.15	0.17	0.20	1.00	2900
	k_std	0.02	0.00	0.02	0.02	0.03	1.00	1100
	k_tau	2500.28	791.71	1372.20	2367.61	4413.45	1.00	1100
	rate	18.40	3.95	12.04	17.89	27.12	1.01	290
	tau	0.12	0.01	0.10	0.12	0.14	1.00	19000
	variance	8.47	0.68	7.24	8.44	9.89	1.00	19000
Model 4	Linf_mu	73.67	5.08	61.87	73.71	83.53	1.00	25000
	Linf_std	15.57	512.36	0.01	0.50	59.34	1.00	65000
	Linf_tau	714.71	2567.91	0.00	3.97	7369.69	1.00	65000
	Shape	32.94	3.68	26.41	32.72	40.80	1.00	17000
	deviance	3988.92	40.17	3913.77	3987.84	4070.70	1.00	57000
	k_mu	0.18	0.03	0.13	0.17	0.23	1.00	50000
	k_std	0.02	0.02	0.01	0.01	0.06	1.00	110000
	k_tau	10041.04	10026.14	286.57	6962.39	37035.94	1.00	110000
	rate	9.40	1.00	7.61	9.35	11.53	1.00	38000
	tau	0.10	0.01	0.09	0.10	0.11	1.00	110000
	variance	10.16	0.74	8.81	10.12	11.72	1.00	110000

Data Source	Model 5	Model 6	Model 7	Model 8	Model 9	Model 10	Model 11
Growth Increment OTP Mark Recapture	X	X	X	X	X	X	X
Direct Aging Ralston & Miyamoto (1983) Integrated Daily Otolith Counts	-	X	X	X	X	-	-
Direct Aging Demartini et al. (1994) Otolith Microincrements	-	X	X	X	X	X	X
Direct Aging Andrews et al. (2012) Bomb Carbon	-	X	X	X	X	X	X
Direct Aging Andrews et al. (2012) Lead:Radium	-	X	X	X	X	X	X
Length Frequency Moffitt & Parrish (1996) Modal Progression	-	X	X	X	X	X	X
Weighting	NA	Equal	By n	Equal	By n	Equal	By n
Pooled Within Data Types?	NA	Yes	Yes	No	No	No	No

Parameter Estiamtes for Integrated Growth Models

	Model 5		Model 6		Model 7		Model 8	
Parameter	**Sample**	**Population**	**Sample**	**Population**	**Sample**	**Population**	**Sample**	**Population**
Linf_mu	62.95	60.98 (56.17, 66.67)	77.96	76.79 (70.27, 78.69)	64.74	64.80 (61.91, 67.17)	66.87	66.89 (63.90, 70.10)
Linf_std	5.07	5.3 (4.53, 6.07)	6.02	5.256 (4.00, 6.83)	5.62	5.57 (4.72, 6.36)	5.53	5.31 (2.61, 6.25)
K	0.275	0.299 (0.229, 0.393)	0.122	0.189 (0.121, 0.235)	0.262	0.260 (0.231, 0.302)	0.253	0.25 (0.21, 0.29)
A_mu	0.98	0.95 (0.8, 1.09)	1.5	1.21 (1.06, 1.50)	1	1.00 (0.92, 1.08)	0.99	0.98 (0.89, 1.10)
A_sig	0.17	0.19 (0.15, 0.24)	0.13	0.16 (0.12, 0.19)	0.18	0.18 (0.14, 0.22)	0.18	0.18 (0.15, 0.21)
Sig	2.5	2.08 (1.50, 2.55)	2.97	2.51 (2.05, 3.11)	2.2	2.20 (1.74, 2.62)	2.32	2.36 (1.94, 2.93)
t0	-	-	-0.86	-0.50 (-0.90, -0.34)	-0.31	-0.32 (-0.44, -0.20)	-0.27	-0.27 (-0.43, -0.17)
oto_sig	-	-	6.79	3.93 (1.31, 7.09)	1.82	1.76 (0.68, 3.03)	1.33	1.30 (0.47, 3.14)
lf_sig	-	-	1.33	3.06 (1.31, 4.06)	4.07	4.39 (3.86, 4.98)	3.93	4.32 (3.53, 5.03)

	Model 9		Model 10		Model 11	
Parameter	**Sample**	**Population**	**Sample**	**Population**	**Sample**	**Population**
Linf_mu	64.74	64.80 (62.22, 67.03)	69.34	68.72 (65.23, 71.68)	68.14	67.55 (65.42, 69.55)
Linf_std	5.62	5.58 (4.74, 6.37)	4.26	4.08 (3.00, 5.11)	4.90	5.00 (4.26, 5.68)
K	0.261	0.26 (0.23, 0.30)	0.146	0.17 (0.13, 0.21)	0.214	0.219 (0.198, 0.245)
A_mu	1	1.00 (0.925, 1.08)	1.5	1.37 (1.19, 1.60)	1.124	1.11 (1.03, 1.19)
A_sig	0.18	0.18 (0.15, 0.22)	0.14	0.155 (0.119, 0.184)	0.16	0.17 (0.14, 0.2)
Sig	2.2	2.20 (1.75, 2.61)	3.29	2.99 (2.45, 3.62)	2.66	2.39 (2, 2.77)
t0	-0.31	-0.32 (-0.43, -0.21)	-0.8	-0.65 (-0.96, -0.43)	-0.37	-0.37 (-0.47, -0.28)
oto_sig	1.82	1.74 (0.66, 2.94)	1.61	1.42 (0.97, 1.84)	1.04	0.96 (0.49, 1.31)
lf_sig	4.07	4.38 (3.88, 4.94)	1.43	2.41 (1.43, 3.29)	3	4.63 (4.15, 5.15)

Model	Linf - Sensitivity	Linf - Original Fit	% Difference in Linf fit	K - Sensitivity	K - Original Fit	% Difference in K fits
Model 1	53.97	61.26	-11.91	0.46	0.3	56.6
Model 2	54.08	61.79	-12.48	0.46	0.29	59.4
Model 3	56.6	73.69	-23.18	0.45	0.17	158.6
Model 4	56.71	73.67	-23.03	0.44	0.18	151.1
Model 5	54.5	62.95	-13.43	0.45	0.27	62.1
Model 6	69.92	77.96	-10.32	0.2	0.12	63.4
Model 7	64.93	64.74	0.29	0.27	0.26	3.6
Model 8	54.5	66.89	-18.53	0.45	0.25	76.1
Model 9	54.5	64.74	-15.82	0.45	0.26	70.7
Model 10	54.5	69.34	-21.41	0.45	0.15	205.1
Model 11	66.47	68.14	-2.45	0.25	0.21	15.5